Pakistan J. Zool., pp 1-10 2024. **DOI**: https://dx.doi.org/10.17582/journal.pjz/20240213050000

Combined Effect of Decellularized Rat Brain Tissue and Nerve Growth Factor on 5 Neural Differentiation of PC12 Cell Line in 2D Cell Culture

Seyed Majid Jalalian Hosseini[1], Javad Baharara[2]*, Shahrbanoo Oryan[3] and Mohammad Amin Kerachian[4,5]

[1]Department of Biology, Science and Research Branch, Islamic Azad University, Tehran, Iran
[2]Department of Biology and Research Center for Animal Development Applied Biology, Mashhad Branch, Islamic Azad University, Mashhad, Iran
[3]Department of Zoology, Faculty of Biological Sciences, Kharazmi University, Tehran, Iran
[4]Department of Chemistry and Biology, Toronto Metropolitan University, Toronto, Canada
[5]Department of Medical Genetics, Faculty of Medicine, University of Medical Sciences, Mashhad, Iran

Article Information
Received 13 February 2024
Revised 25 February 2024
Accepted 12 March 2024
Available online 23 May 2024
(early access)

Authors' Contribution
SMJH, JB and SHO designed the study, performed and facilitated the experiments, statistical analysis, wrote the protocol and manuscript. JB and SHO sample collection, critically reviewed the manuscript and finalized it. MAK helped in lab work and statistical analysis. All authors read and approved the final manuscript.

Key words
Nerve growth factor, Nestin, β-tubulin III, PC12 cell, Decellularized rat brain, Neural differentiation

ABSTRACT

Recent advancements in tissue engineering suggest that biomaterials, particularly decellularized extracellular matrix (ECM), have the potential to improve the targeting and effectiveness of regenerative therapies in the central nervous system. In present experimental study utilized powder derived from a decellularized rat brain tissue scaffold combined with a growth factor. PC12 cells were exposed to nerve growth factor (NGF) and dECM in a two-dimensional cell culture. Cell proliferation rate and percentage of viable cells were evaluated using trypan blue, while samples were stained with DAPI and cresyl violet. The mRNA expression patterns associated with nerve cell differentiation post-extraction were measured using the qRT-PCR method, and cell differentiation was assessed through immunocytochemical evaluation. The findings revealed that the differentiated PC12 cells exhibited a higher level of mRNA compared to the control cells. A statistically significant increase in mRNA level was observed for Nestin and β-tubulin III. Furthermore, the immunocytochemistry results showed that the differentiated PC12 cells expressed a higher level of these proteins compared to the control cells. The evaluation of neuronal differentiation induction in PC12 cells in two-dimensional conditions revealed a significant increase in the expression of neural differentiation biomarkers Nestin and β-Tubulin III in the treatment groups compared to the control group. This suggests that the combined effect of decellularized rat brain tissue powder and NGF can be considered an inducer of neural differentiation in PC12 cells.

INTRODUCTION

Disease is an abnormal condition that affects a part of the body or the whole body and leads to a series of mild to severe symptoms (Abbaszadeh *et al*., 2019; Aidy *et al*., 2020; Anbari *et al*., 2019; Basati *et al*., 2020). The spread of chronic and non-infectious diseases is one of the current medical problems (Ebrahimi *et al*., 2019; Hassanzadeh *et al*., 2023; Kaliwal *et al*., 2006; Mussavi *et al*., 2014; Shi *et al*., 2021). Currently, peripheral nerve damage affects over a million individuals across the globe. The management of this condition remains challenging, as a significant number of treatments show effectiveness in just 50% of patients. The increasing elderly population on a global scale, combined with a higher prevalence of non-communicable diseases (NCDs) is driving the demand for therapeutic interventions that can effectively address the loss of degenerative tissue (Lin *et al*., 2018). A

* Corresponding author: baharara78@gmail.com
0030-9923/2024/0001-0001 $ 9.00/0

promising approach in tissue engineering involves the use of decellularized scaffolds, which offer advantages such as aiding tissue repair and lacking immunogenicity compared to artificial scaffolds. Simplifying tissue engineering techniques may be crucial for restoring damaged nerve tissues, for instance through the preparation of decellularized scaffolds and utilization of 3D culture methods (Moxon *et al*., 2019). Natural extracellular matrix (ECM) proteins offer an alternative to complex engineered scaffolds. They are highly suitable for tissue regeneration due to their composition and structure, which closely resemble the natural environment of cells. Therefore, decellularized human tissue pieces can be viewed as porous three-dimensional scaffolds with architecture akin to natural tissue ECM (Forraz *et al*., 2013).

The PC12 cell line is commonly used in neuroscience research to study neuroprotection, neurosecretion, neuroinflammation, and synaptogenesis (Darbinian, 2013). In the scientific community, floating cells influenced by nerve growth factor (NGF) are considered similar to cortical neurons, and their use in studying the physiology and pathology of the nervous system is recommended. NGF concentrations increase at the site of nerve injury, prompting Schwann cells to produce more NGF receptors, which deliver the growth factor to axonal extensions (Sultan *et al*., 2021). The β-tubulin III protein is predominantly found in neurons and testicular cells and is encoded by the TUBB3 gene. Inactivation of the TUBB3 gene disrupts neural progenitor proliferation (Lazzarini *et al*., 2019). Nestin, a type VI intermediate filament protein, is a key component of the cytoskeleton in stem cells and plays a role in their functions, including proliferation, differentiation, and migration (Bernal and Arranz, 2018). It is also essential for the proliferation of neural progenitor cells in the embryonic cortex and is expressed in the early stages of neurogenesis as a marker of neuroectoderm stem cells and neural progenitor cells (Liu *et al*., 2021). The present experimental research aimed to evaluate the decellularized brain tissue in conjunction with NGF and its ability to stimulate neuronal adhesion and proliferation via *in vitro* investigations using PC12 cells to apply the findings to enhance neural tissue engineering techniques.

MATERIALS AND METHODS

Laboratory animal

Twenty-four male Wistar rats (two months old; weight: 230 ± 20 g) were purchased and kept in standard cages (Jabbari *et al*. 2020).

Decellularization and preparation of decellularized matrix solution

Adult rats were euthanized with Ketamine 100 mg/Kg and Xylazine 10 mg/Kg by intraperitoneal injection and brain tissues were isolated by splitting the skull from the occipital region. Subsequently, the tissues were decellularized using a chemical method. Briefly, the collected tissues were first immersed in deionized water, then added a 3% Triton X-100 solution (Sigma), followed by deionized water, and subsequently in a 4% sodium deoxycholic acid solution (Sigma). This was followed by another round of deionized water (10 min, repeated 3 times). In the final washing step, brain samples were kept at 4°C in PBS (Gibco) containing 1% penicillin antibiotic. All decellularization procedures were conducted using a shaker incubator at 120 rpm at room temperature. To eliminate any remaining detergents from the decellularized tissue, it was immersed in PBS for 3 days, followed by a solution of 0.1% acetic acid in 4% ethanol for 4 h. Afterward, it was rinsed with sterile PBS, placed near liquid nitrogen, and ultimately subjected to freeze-drying using a freeze-dryer (Pishtaz-Iran) to produce decellularized extracellular matrix (dECM) powder (Liu *et al*., 2021). The dECM powder was mixed with acetic acid and pepsin (in a 1:10 ratio) and kept at room temperature for 48 h. After dissolving PBS, the dECM solution was then filtered through a 40 µm filter to remove any remaining particles and stored at 20 °C for further experiments (Jang *et al*., 2017).

Confirmation analyses of decellularization

To confirm proper decellularization and remove cells from the scaffolds, portions of the decellularized and control brain samples were rinsed in distilled water after being fixed at room temperature, dehydrated in graded alcohol, and paraffin molds were created from the samples using a microtome. Sections of 5 µm were prepared, followed by an assessment of tissue staining protocols, electron micrographs, and DNA content (Jang *et al*., 2017).

Tissue staining

Brain samples were fixed in 4% paraformaldehyde (Sigma) for 24 h at 4°C. They were then washed with distilled water, dried in graded alcohol, and paraffinized. A 5 µm section was prepared, and slides were deparaffinized and hydrated, followed by immersion in hematoxylin dye (Sigma) for 7 sec. After a 1 min wash in distilled water, they were placed in lithium carbonate (Sigma) for 2 sec, and then in eosin dye (Sigma) for 3 min. Finally, the samples were evaluated using a light microscope (Sharifnia *et al*., 2023).

Sections were deparaffinized and hydrated, then stained with the nucleic acid fluorescent dye DAPI, which binds strongly to adenine-thymine-rich regions in DNA. After that, they were incubated for 20 min at

room temperature in darkness and compared with control samples using a fluorescent microscope (Crapo *et al*., 2014).

To analyze the remaining glycosaminoglycans, we utilized periodic acid-Schiff staining. Initially, deparaffinized and hydrated sections were treated with 4% paraformaldehyde for 5 min, followed by two washes with PBS. Subsequently, the sections were exposed to a periodic acid solution for 5 min. Then, they were immersed in Schiff's reagent (Sigma) for 15 min. After drying, a coverslip was placed on the samples for further evaluation using an optical microscope (Liu *et al*., 2021).

Scanning electron micrographs (SEM)

Normal and decellularized rat brain tissue samples were fixed in 2.5% glutaraldehyde for 20 min, washed with PBS, and prepared for SEM. Following drying, the samples were coated with gold-palladium for 180 sec using a sc7620 sputter coater and then imaged with a 1450VP scanning electron microscope (LEO-Germany) at various magnifications with a resolution of 2.5 nm (Jabbari *et al*., 2020).

Evaluation of DNA content

To verify the accuracy of decellularization, the genomic DNA of both decellularized samples and normal brain tissue was extracted and the concentration was determined. The percentage of cells removed from the decellularized tissues was then compared. First, small fragments of (10-15 mg) weight of normal tissue and decellularized tissue from the rat brain were divided into micro tubes. The genomic DNA of the samples was extracted using a column DNA extraction kit (Denazist, Iran). To ensure the quality and quantity of the DNA, the samples were checked on 1% agarose gel, and the concentration was measured with an Epoch spectrophotometer (BioTek - USA) (Crapo *et al*., 2014).

PC12 cells culture

The PC12 cell line consists of round, suspended cells obtained from the Pasteur Institute cell bank (ATCC; CRL-1721, Tehran, Iran). These cells were cultured in RPMI1640 medium with 15% fetal bovine serum (FBS) and 1% penicillin/streptomycin (PS) in an incubator set at 37°C with 5% carbon dioxide and 90% humidity. Approximately 0.5×10^6 cells were counted and centrifuged for 3 min at 1200 rpm. The cell sediment was then resuspended in a culture medium containing 5% DMSO and poured into special vials for freezing. The vials were initially placed in a freezer at - 80°C and then transferred to a liquid nitrogen tank at - 196°C for 24 h (Wiatrak *et al*., 2020). The frozen PC12 cells were thawed by placing them in a Bain-Marie at 37°C, then transfered to a sterile tube with 5 mL of RPMI1640 medium and 10% FBS. The cells were centrifuged and the sediment was suspended for 3 min at 1200 rpm in flasks or 6-well plates. After 48 h of culturing in the flasks, the PC12 cells started to form colonies, leading to the formation of embryonic bodies and the cells becoming spheroids. These spheroids were used for tests both in two-dimensional differentiation environments and 3D settings (Abe *et al*., 2015).

Neural differentiation of PC12 cells

PC12 cells were cultured in T25 polystyrene flasks with RPMI complete culture medium for one week, and the medium was changed every 48 h according to the following grouping. Control group: PC12 cell; experimental group 1: PC12 cells treated with NGF (50 ng/mL); experimental group 2: PC12 cells treated with dECM (500 µg/mL); experimental group 3: PC12 cells and treatment with NGF and dECM.

Morphological evaluation

Morphological examination, the cells in the scaffold were carefully evaluated by inverted microscope with 200X magnification and the process of differentiating changes in the research groups was imaged as well as the morphology of the cells using hematoxylin and eosin staining was also examined and the percentage of living cells determined (Yousefi *et al*., 2021).

Cresyl violet staining

To examine the emergence of neurons resulting from the differentiation of primary cells, a specific staining technique called cresyl violet staining (Merck) was employed. This staining method targets Nissl bodies within neurons, resulting in a distinct purple coloration. Following the staining process, cells that exhibit a positive response to cresyl violet will exhibit a purple hue. The cells were initially placed in a 4% paraformaldehyde solution for 5 min. Subsequently, they were washed with PBS and fixed in 70% ethanol for 10 min at room temperature. Finally, the cells were exposed to a cresyl violet solution containing cresyl violet (0.25%), glacial acetic acid (0.8%), sodium acetate (0.6 mM), and distilled water (100 mL) for a period ranging from three to 10 min. Once the staining process was complete, the cells were photographed and observed under an optical microscope.

Molecular assessment of gene expression

The PC12 cells from both the treatment and control groups were separated from the differentiation medium and scaffold at the end of the second week. Subsequently, RNA extraction was performed followed by cDNA synthesis using specific primers for β-tubulin III and Nestin genes. The qPCR method was used to measure the

expression levels of these genes based on previous studies. The primers were designed using Oligo 7 software and their specificity was confirmed through a BLAST search using the NCBI database (Gheibi *et al*., 2020). It should be noted that the mRNA expression of the examined genes was normalized with the mRNA expression of the internal control gene and the fold change was calculated using the formula $^{-2\Delta\Delta}$Ct (Table I).

Table I. Primers used in this study.

Primer name	Sequence 5'→ 3' (10-50 bp)	Length	Amplicon size (bp)
Rpl19 F	GGCTCGATGCCGGAAGAACA	20	283
R	TAGCTTCTTGCGGGCCTTGT	20	
Tubb3 F	TATGTGGGGGACTCGGACCT	20	387
R	GTCAGGGTACTCCTCACGCAC	21	
Nes F	CTGGCACACCTCAAGAT-GTCCCTTAGTCTG	30	159
R	CTCTGGTATCCCAAGGAAAT-TCGGCTTC	28	

Immunocytochemistry (ICC) evaluation

To assess the neural differentiation of PC12 cells, we utilized an immunocytochemical technique to investigate the expression of neural markers, such as Nestin and β-tubulin III. The method involved identifying and displaying specific proteins in antigen-antibody reactions. Initially, the supernatant medium was removed, and the samples were fixed with 4% paraformaldehyde in PBS for 20 min. Subsequently, the samples underwent a series of three 5-min washes. Following this, 0.3% Triton was applied for 30 min to permeabilize the cell membrane, and the samples were then washed with PBS. To prevent the secondary antibody reaction, 10% goat serum was added for 45 min. After removing the goat serum, Nestin primary antibody (Biorbyt-orb251614) and β-tubulin III primary antibody (Biorbyt-orb555945), both diluted (1 to 100) with PBS, were applied to the samples and refrigerated at 2 degrees for 24 h. Subsequently, the samples were washed four times with PBS for 5 min each, and the secondary antibody Goat Anti-Rabbit IgG (H+L) antibody (FITC) (Biorbyt-orb688925) was added at a 1 to 150 dilution and incubated at 37 degrees for 1 h and 30 min in the dark. After transferring the sample from the incubator to a dark room and performing three washes, DAPI was added, followed by a final wash with PBS, and fluorescent photography was conducted (Agarwal *et al*., 2022).

Statistical analysis

Data analysis was performed using Graph-Pad Prism statistical software version 8. RT-PCR data were analyzed using REST. The One-way ANOVA method and Tukey's multiple comparison test were used to compare the results of different groups. P value less than 0.05 was considered significant level of difference in this study to compare the model group with treatment groups. The asterisks replicate significant differences with *: $p<0.05$, **: $p<0.01$, and ***: $p<0.001$.

RESULTS

Tissue staining confirmed successful decellularization. Figure 1 shows the nuclei turned purple with hematoxylin, while the cytoplasm turned red with eosin. The decellularization process was effective.

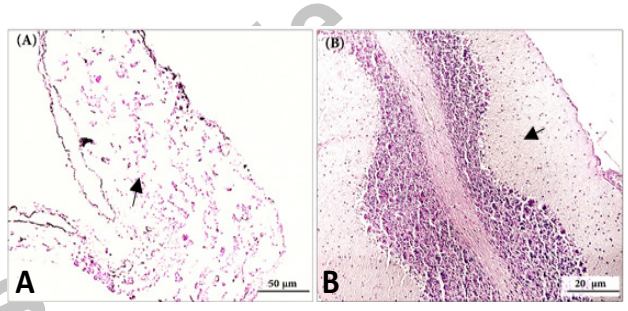

Fig. 1. Microscopic images of hematoxylin and eosin staining of decellularized tissue and control rat brain. (A) Decellularized brain tissue of rat brain, matrix remnants are discernible after removal of nuclei (arrow). Scale bar 50 µm. (B) Image of normal rat brain tissue, nuclei are seen darker (arrow) Magnification (A) X40, (B) X100 Scale bar 20 µm.

This staining in Figure 2 was used to stain the nuclei and confirm the removal of cells from the decellularization scaffolds. In this method, fluorescent dye was attached to regions of DNA. Comparing the images of experimental and control groups determined that decellularization caused the removal of brain tissue cells and the quality was appropriate.

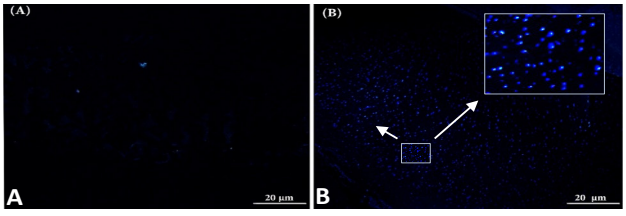

Fig. 2. Microscopic images of DAPI fluorescent staining of decellularized tissue and control rat brain. (A) Decellularized rat brain tissue, scale bar 20 µm. (B) Image of normal rat brain tissue, arrow shows one of the nuclei. Magnification X100, scale bar 20 µm.

To assess the quality of the remaining glycosaminoglycans (GAGs), the periodic acid-Schiff staining was carried out. Upon comparing the images obtained (Fig. 3), it is evident that the decellularization process was executed with commendable proficiency, resulting in the preservation of a substantial quantity of extracellular matrix.

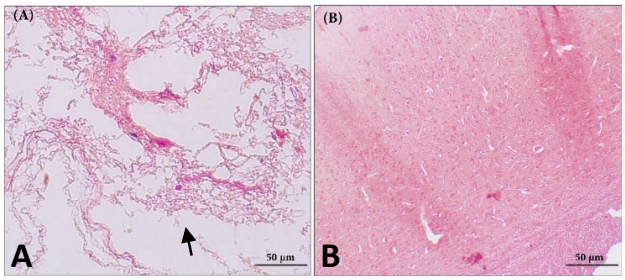

Fig. 3. Microscopic images of periodic acid-Schiff staining of decellularized tissue and control rat brain. (A) Decellularized rat brain tissue, arrow indicates preserved extracellular matrix. Scale bar 50 µm. (B) Image of normal rat brain tissue, magnification X100, and scale bar 50 µm.

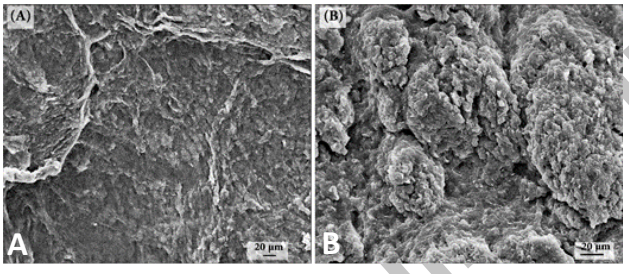

Fig. 4. Scanning electron micrographs of decellularized and control rat brain tissue. (A) Decellularized brain, scale bar 20 µm. (B) Image of normal rat brain tissue, magnification X1000, scale bar 20 µm.

Scanning electron micrographs were prepared from decellularized and control rat brain tissue (Fig. 4). The analysis of the decellularized brain reveals a three-dimensional network architecture devoid of cellular components, yet characterized by the presence of pores that result from the compression of the brain matrix layers. The comparison of the images shows that the decellularization has been done properly.

This investigation demonstrated that the quantity of genomic DNA in the decellularized sample was decreased by approximately 90% when compared to the control sample, and this decrease was statistically significant ($p<0.05$), thereby validating the appropriateness of the decellularization process. Furthermore, the integrity of the DNA samples was assessed via a 1% agarose gel (Fig. 5).

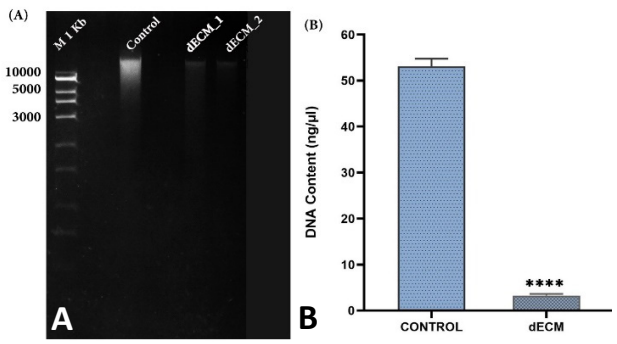

Fig. 5. Evaluation of genomic DNA content of decellularized tissue and control rat brain. (A) Quality of genomic DNA content extracted on agarose gel. (B) Comparison of the extracted DNA concentration of the decellularized group and the normal rat brain tissue shows a decrease of about 90% and is significant at the ($p<0.0001$) level.

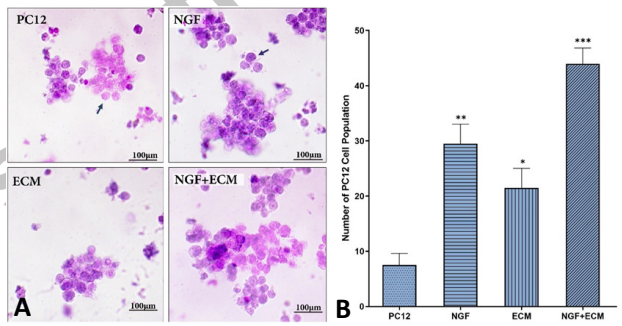

Fig. 6. Confirmation of the formation of Nissl bodies by cresyl violet staining in two-dimensional culture conditions. (A) Light microscopic images of cresyl violet-stained PC12 cells in two-dimensional arrays (arrows indicate unresponsive PC12 cells) (3 replicates, X200 magnification, scale bar 100 µm). (B) Mean (SD ± SD) of PC12 cells positive for Nissl bodies 7 days after treatment shows, there was a significant difference between the treatment groups and the control group ($p < 0.05$; 3 replicates).

The average percentage of cells differentiated to neuron-like cells in 2D culture in all treatment groups was higher than the control group. As shown in Figure 7, the number of cell differentiated in the NGF+dECM group was higher than the control group ($p<0.001$). Additionally, a significant changes were observed in the treated groups with NGF ($p<0.01$) and dECM ($p<0.05$) compared with the control group.

The results of Nestin gene expression in a 2D culture medium indicated augmented expression in all treatment groups compared to the control group. This increase was significant for the NGF treatment group ($p<0.05$) and the combined NGF+ECM treatment group showed an even

higher level ($p<0.0001$) (Figs. 6 and 7A). Additionally, the results of β-Tubulin III gene expression revealed a significant increase in all treatment groups compared to the control group. However, it exhibited a different pattern than Nestin, with the NGF treatment group showing a much higher rise in expression compared to the other treatment groups ($p<0.0001$) (Fig. 7B).

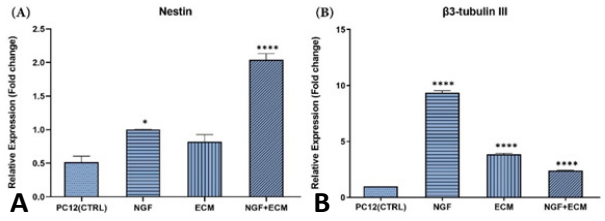

Fig. 7. Comparison of mean expression changes of Nestin and β-Tubulin III genes seven days after treatment in two-dimensional culture conditions ($p<0.05$; 3 independent replicates). (A) Nestin gene expression changes were significantly increased in the ECM treatment group and NGF+ECM group compared to the PC12 control group. (B) β-Tubulin III gene expression changes in two-dimensional culture compared to the PC12 control group in all treatment groups including the NGF group, ECM group, and NGF+ECM group had a significant increase (**** is significant at $p<0.0001$ level) * is significant at $p<0.05$ level).

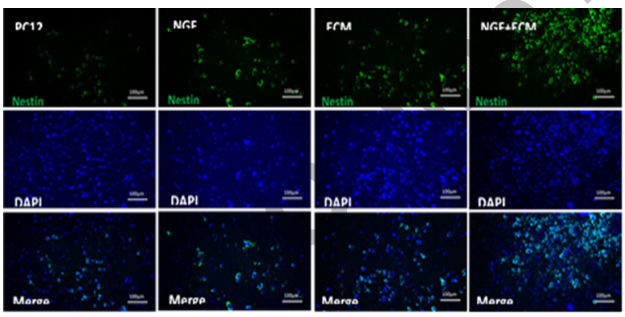

Fig. 8. Immunocytochemical staining of Nestin biomarker in two-dimensional culture. Neuronal specific biomarker protein expression Nestin in treatment and control groups, 7 days after the start of treatment. All nuclei were stained with DAPI (magnification X200, scale bar 100 µm; replicate 3).

The results of two-dimensional culture showed that the mean percentage of expression of Nestin and β-Tubulin III in PC12 cells in all treatment groups 7 days after the start of treatment increased significantly compared to the control group (Figs. 8-10). The results obtained from the immunofluorescence assessment of the expression of Nestin showed a significant increase following NGF+ECM treatment in the PC12 cells as compared to the control ($p<0.001$). Moreover, the expression of Nestin significantly augmented in NGF ($p<0.01$), and ECM ($p<0.01$) treated groups as compared to the control group (Fig. 9). On the contrary, the outcomes obtained from the evaluation of β-Tubulin III expression through immunofluorescence analysis exhibited a notable increase after the application of NGF+ECM treatment in the PC12 cells in comparison to the control group ($p<0.01$). Additionally, the expression of β-Tubulin III significantly amplified in the NGF ($p<0.05$) and ECM ($p<0.05$) treated groups about the control group (Fig. 9).

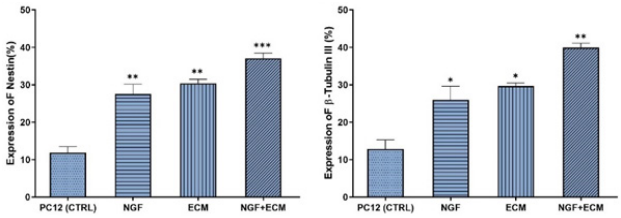

Fig. 9. Comparison of the mean protein expression percentage of neural biomarkers 7 days after treatment in 2D culture conditions ($p<0.05$; 3 independent replicates). (A) The mean percentage of Nestin protein expression showed a significant increase in the NGF+ECM group compared to the PC12 control group. (B) The mean percentage of β-Tubulin III protein expression in two-dimensional culture significantly increased compared to the control group of PC12 in the treatment groups. It showed that the combined treatment group (NGF+ECM) had a greater increase than the other treatment groups *** in the level $p<0.001$ is significant. * is significant at $p<0.05$ level).

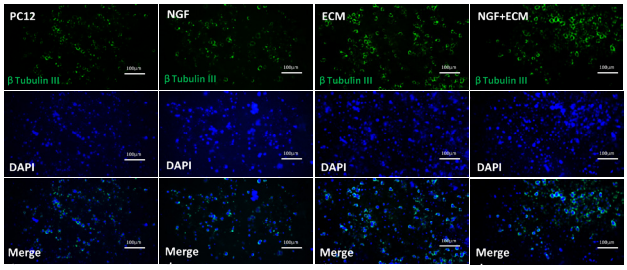

Fig. 10. Immunocytochemical staining of β-Tubulin III biomarker in two-dimensional culture. Neuronal specific biomarker β-Tubulin III protein expression in treatment and control groups, 7 days after the start of treatment. All nuclei were stained with DAPI (magnification X200, scale bar 100 µm; replicate 3).

DISCUSSION

Results showed higher mRNA levels in treated

PC12 cells. Nestin gene expression increased in all groups, but not significantly in some due to timing. B-tubulin III gene expression was higher during extraction. Test groups mRNA correlated with β-tubulin III gene expression, indicating neural progenitor cell differentiation. Immunocytochemistry revealed higher protein levels in treated PC12 cells, suggesting neural induction. Morphological analysis showed changes in cell morphology and neurite development. Cell differentiation assessment in treatment groups aligns with other studies. The therapeutic strategies of neural tissue engineering are different based on the type of neural tissue damage. It is important to note that while the principles of neural tissue engineering encompass the three main components of cells, growth factors, and scaffolds, the design of models must also consider many other factors due to the significance of the nervous system. These include differences between the central nervous system (CNS) and the peripheral nervous system (PNS) in terms of restoration and stem cells, precise control of environmental conditions, attention to electrical activity, cell orientation and communication, unique conditions of the central nervous system, release of nerve agents, and the importance of supporting cells for neurons (Mobini *et al*., 2019; Yang *et al*., 2021; George *et al*., 2020).

Gębczak and his colleagues investigated the effect of a decellularized commercial matrix on survival, proliferation and migration of PC12 cell line. The scaffold reduced the percentage of apoptosis and necrosis and stimulated proliferation and possibly migration of PC12 cells (Gębczak *et al*., 2021). The PC12 cells used in this research were of the suspension type, which have a tendency to accumulate and adhere weakly to uncoated surfaces. It has been determined that these cells originate from the pheochromocytoma located in the medulla of the rat adrenal gland and are considered a suitable model for investigating the differentiating effects of diverse factors (Crapo *et al*., 2014). Recently, there has been a notable advancement in neural tissue engineering strategies aimed at repairing damaged nerves and neural tissues. Specifically, the focus has been on the development of neural scaffolds that mimic the extracellular matrix to provide structural and biochemical cues for promoting neural regeneration. The ideal materials for implantation in nerve tissue repair are biodegradable and bioabsorbable, such as 3D bioscaffolds, which can serve as support structures for both endogenous and exogenous stem cells (Forraz *et al*., 2013).

Growth factors are soluble signaling molecules that control cellular responses through specific binding of receptors on target cells. Numerous studies have shown the positive effect of these factors in the repair of the spinal cord and brain. This factor triggers neural differentiation reactions in PC 12 cells which has the dual biological role of promoting axon growth. Therefore, it can play an important role in the signal transmission system and control neural growth. Among the neurotrophic factors, the most studies have been conducted for the treatment of peripheral nerve damage using NGF. One of the goals of tissue engineering is the development of various biomaterials containing NGF. As a result of the presence of NGF, the number of mature nerve fibers increases, resulting in better functional improvement, including the speed of nerve transmission, compared to control groups. Also, in the presence of NGF, the diameter of the axons in the conduits was larger than the channels without NGF (Belanger *et al*., 2016). Previous studied showed that the treatment of PC12 cells with neurotrophic factors increases the expression of neuronal markers Nestin and β-Tubulin III and plays a role in the survival and stimulation of neurons growth (Sultan *et al*., 2021).

Morphological studies also support the evidence of differentiation of PC12 cells into neuron-like cells. However, the expression of a few neuronal proteins is not enough to claim that these cells are capable of performing the complex functions of mature neurons. Therefore, more studies are needed to investigate the function of these cells and their electrophysiological properties. Nissl bodies in PC12 cells indicate neural differentiation and can be identified by specific cresyl violet staining. The results indicated a significant increase in the average number of cells differentiating into neuron-like cells in all treatment groups compared to the control group (Marei *et al*., 2018). Lazzarini *et al*. (2019) showed morphological and biochemical changes in the neural induction of mesenchymal stem cells and pointed out the expression of neural markers such as Nestin and β-tubulin III and considered their high expression related to neural differentiation. It has also been found that the increased expression of neuronal markers Nestin and β-Tubulin III is associated with the growth of neurites (Lazzarini *et al*., 2019). Also, in a study, Marei and his colleagues treated mesenchymal stem cells with neural induction media and based on morphological changes and qPCR, differentiated mesenchymal stem cells expressed markers for immature and mature neurons. β-tubulin III and MAP2 respectively show the neural potential of these cells to differentiate into functional neurons (Marei *et al*., 2018).

Nestin is an intermediate strand protein known as a marker of neural stem/progenitor cells. B-tubulin III is a microtubule element of the tubulin family that is found almost exclusively in neurons involved in axon guidance and maintenance, an essential step in neurogenesis, especially in dendrites, which has a role in determining

and stabilizing dendritic shape during neuron growth. β-Tubulin III is a key neuronal marker that plays a role in the production, guidance and maintenance of neurites during neurogenesis (Lazzarini *et al*., 2019). Moxon *et al*. (2019) showed that increased expression of β-Tubulin III was associated with neurite growth. Bernal and Arranz (2018) showed that Nestin is a neuron-specific biomarker that is essential in the proliferation of neural progenitor cells in the central nervous system, the higher the level of Nestin expression indicates the progress in transforming progenitor cells into neural cells (Bernal and Arranz, 2018). Previous research developed a biofunctional electrospun fibrous mesh (eFM) by selectively retrieving NGF from rat blood plasma. The neurite outgrowth induced by the eFM-NGF systems was assessed by culturing PC12 cells for 7 days, without medium supplementation. The biological results demonstrated that NGF delivery system stimulates neuronal differentiation, enhancing neurite growth more than the control condition (Casanova *et al*., 2021). The results of real time-PCR showed that the differentiated PC12 cells express a higher level of mRNA than the control cells. The current study's findings on the creation of decellularization powder from rat brain tissue indicate successful decellularization and lyophilized powder preparation, as determined through qualitative and quantitative evaluations based on existing standards. Additionally, the evaluation of neuronal differentiation induction in PC12 cells under two-dimensional conditions revealed a significant increase in the expression of neural differentiation biomarkers Nestin and β-Tubulin III in the treatment groups compared to the control group. This suggests that the combined effect of decellularized rat brain tissue powder and growth factor NGF can be considered an inducer of neural differentiation in PC12 cells.

DECLARATIONS

Acknowledgement

This study constitutes an integral component of the Ph.D. thesis undertaken by SMJH at Islamic Azad University, Tehran, Iran. The authors extend their heartfelt gratitude to the Research Center for Applied Biology of Animal Development, Islamic Azad University of Mashhad, and the Stem Cells and Regenerative Medicine Research group at the Academic Center for Education, Culture, and Research, Khorasan Razavi, for their invaluable assistance and support throughout this research endeavor.

Funding

The study received no external funding.

Ethics statement

The National Committee for Research Ethics of Islamic Azad University, Tehran, Iran, approved all animal experimental procedures and care (Ethical code: ID IR.IAU.SRB.REC.1398.058).

Availability of data and material

The datasets used or analyzed during the current study are available from the corresponding author on reasonable request.

Statement of conflict of interest

The authors have declared no conflict of interest.

REFERENCES

Abbaszadeh, S., Teimouri, H. and Farzan, B., 2019. An ethnobotanical study of medicinal plants with antianxiety and antidepressant effects in Shahrekord. *Egypt. J. Vet. Sci*., **50**: 81-87. https://doi.org/10.21608/ejvs.2019.12612.1077

Abe, H., Ino, K., Li, C.Z., Kanno, Y., Inoue, K.Y., Suda, A., Kunikata, R., Matsudaira, M., Takahashi, Y., Shiku, H. and Matsue, T., 2015. Electrochemical imaging of dopamine release from three-dimensional-cultured PC12 cells using large-scale integration-based amperometric sensors. *Anal. Chem*., **87**: 6364–6370. https://doi.org/10.1021/acs.analchem.5b01307

Agarwal, G., Roy, A., Kumar, H. and Srivastava, A., 2022. Graphene-collagen cryogel controls neuroinflammation and fosters accelerated axonal regeneration in spinal cord injury. *Biomater. Adv*., **139**: 212971. https://doi.org/10.1016/j.bioadv.2022.212971

Aidy, A., Karimi, E., Ghaneialvar, H., Mohammadpour, S. and Abbasi, N., 2020. Protective effect of Nectaroscordum tripedale extract and its bioactive component tetramethylpyrazine against acetaminophen-induced hepatotoxicity in rats. *Adv. Tradit. Med*., **20**: 471-477. https://doi.org/10.1007/s13596-020-00431-z

Anbari, K., Hasanvand, A., Andevari, A.N. and Abbaszadeh, S., 2019. Concise overview: A review on natural antioxidants and important herbal plants on gastrointestinal system. *Res. J. Pharm. Technol*., **12**: 841-847. https://doi.org/10.5958/0974-360X.2019.00145.8

Basati, G., Ghanadi, P. and Abbaszadeh, S., 2020. A review of the most important natural antioxidants and effective medicinal plants in traditional medicine on prostate cancer and its disorders. *J. Herbmed Pharmacol*., **9**: 112-120. https://doi.org/10.34172/jhp.2020.15

Belanger, K., Dinis, T.M., Taourirt, S., Vidal, G., Kaplan, D.L. and Egles, C., 2016. Recent strategies in tissue engineering for guided peripheral nerve regeneration. *Macromol. Biosci*., **16**: 472–481. https://doi.org/10.1002/mabi.201500367

Bernal, A. and Arranz, L., 2018. Nestin-expressing progenitor cells: Function, identity and therapeutic implications. *Cell. Mol. Life Sci*., **75**: 2177–2195. https://doi.org/10.1007/s00018-018-2794-z

Casanova, M.R., Reis, R.L., Martins, A. and Neves, N.M., 2021. Stimulation of neurite outgrowth using autologous, NGF bound at the surface of a fibrous substrate. *Biomolecules*, **12**: 25. https://doi.org/10.3390/biom12010025

Crapo, P.M., Tottey, S., Slivka, P.F. and Badylak, S.F., 2014. Effects of biologic scaffolds on human stem cells and implications for CNS tissue engineering. *Tissue Eng. A*, **20**: 313–323. https://doi.org/10.1089/ten.tea.2013.0186

Darbinian, N., 2013. Cultured cell line models of neuronal differentiation: NT2, PC12. *Methods Mol. Biol*., **1078**: 23–33. https://doi.org/10.1007/978-1-62703-640-5_3

Ebrahimi, Y., Hasanvand, A., Valibeik, A., Ebrahimi, F. and Abbaszadeh, S., 2019. Natural antioxidants and medicinal plants effective on hyperlipidemia. *Res. J. Pharm. Technol*., **12**: 1457-1462. https://doi.org/10.5958/0974-360X.2019.00242.7

Forraz, N., Wright, K.E., Jurga, M. and McGuckin, C.P., 2013. Experimental therapies for repair of the central nervous system: stem cells and tissue engineering. *J. Tissue Eng. Regen. Med*., **7**: 523–536. https://doi.org/10.1002/term.552

Gębczak, K., Wiatrak, B. and Fortuna, W., 2021. Evaluation of PC12 cells proliferation, adhesion and migration with the use of an extracellular matrix (CorMatrix) for application in neural tissue engineering. *Materials*, **14**: 3858. https://doi.org/10.3390/ma14143858

George, J., Hsu, C.C., Nguyen, L.T.B., Ye, H. and Cui, Z., 2020. Neural tissue engineering with structured hydrogels in CNS models and therapies. *Biotechnol. Adv*., **42**: 107370. https://doi.org/10.1016/j.biotechadv.2019.03.009

Gheibi, P., Eftekhari, Z., Doroud, D. and Parivar, K., 2020. Chlorpyrifos effects on integrin alpha v and beta 3 in implantation window phase. *Environ. Sci. Pollut. Res*., **27**: 29530–29538. https://doi.org/10.1007/s11356-020-08288-0

Hassanzadeh, K.H., Mohammad, A.A., Yousif, R.S., Jasim, S.A., Kzar, H.H., Lafta, M.H., Jalil, A.T., Romero Parra, R.M. and Darvishi, M., 2023. SARS-CoV2 neuroinvasive potential in respiratory failure in COVID-19 patients. *Caspian J. environ. Sci.*, **21**: 467-472.

Jabbari, N., Eftekhari, Z., Roodbari, N.H. and Parivar, K., 2020. Evaluation of encapsulated eugenol by chitosan nanoparticles on the aggressive model of rheumatoid arthritis. *Int. Immunopharmacol*., **85**: 106554. https://doi.org/10.1016/j.intimp.2020.106554

Jang, J., Park, H.J., Kim, S.W., Kim, H., Park, J.Y., Na, S.J., Kim, H.J., Park, M.N., Choi, S.H., Park, S.H. and Kim, S.W., 2017. 3D printed complex tissue construct using stem cell-laden decellularized extracellular matrix bioinks for cardiac repair. *Biomaterials*, **112**: 264–274. https://doi.org/10.1016/j.biomaterials.2016.10.026

Kaliwal, B.B. and Ksheerasagar, R.L., 2006. Histological and biochemical changes in the liver of albino mice on exposure to insecticide, carbosulfan. *Caspian J. environ. Sci.*, **4**: 67-76.

Lazzarini, R., Guarnieri, S., Fulgenzi, G., Mariggiò, M.A., Graciotti, L., Martiniani, M., Orciani, M., Specchia, N. and Di Primio, R., 2019. Mesenchymal stem cells from nucleus pulposus and neural differentiation potential: A continuous challenge. *J. mol. Neurosci*., **67**: 111–124. https://doi.org/10.1007/s12031-018-1216-x

Lin, T., Liu, S., Chen, S., Qiu, S., Rao, Z., Liu, J., Zhu, S., Yan, L., Mao, H., Zhu, Q. and Quan, D., 2018. Hydrogel derived from porcine decellularized nerve tissue as a promising biomaterial for repairing peripheral nerve defects. *Acta Biomater*., **73**: 326–338. https://doi.org/10.1016/j.actbio.2018.04.001

Liu, Y., Zou, L., Wang, P., Zhou, J., Yuan, C. and Wang, J., 2021. Construction of differential expression plasmids of NGF to detect its influence on PC12 cell neuronal differentiation. *Exp. Ther. Med*., **21**: 363. https://doi.org/10.3892/etm.2021.9794

Marei, H.E.S., El-Gamal, A., Althani, A., Afifi, N., Abd-Elmaksoud, A., Farag, A., Cenciarelli, C., Thomas, C. and Anwarul, H., 2018. Cholinergic and dopaminergic neuronal differentiation of human adipose tissue derived mesenchymal stem cells. *J. cell. Physiol*., **233**: 936–945. https://doi.org/10.1002/jcp.25937

Mobini, S., Song, Y.H., McCrary, M.W. and Schmidt, C.E., 2019. Advances in ex vivo models and lab-on-a-chip devices for neural tissue engineering. *Biomaterials*, **198**: 146–166. https://doi.org/10.1016/j.biomaterials.2018.05.012

Moxon, S.R., Corbett, N.J., Fisher, K., Potjewyd, G., Domingos, M. and Hooper, N.M., 2019. Blended,

alginate/collagen hydrogels promote neurogenesis and neuronal maturation. *Mater. Sci. Eng. C. Mater. Biol. Appl.*, **104**: 109904. https://doi.org/10.1016/j.msec.2019.109904

Mussavi, M., Asadollahi, K., Janbaz, F., Mansoori, E. and Abbasi, N., 2014. The evaluation of red reflex sensitivity and specificity test among neonates in different conditions. *Iran. J. Pediat.*, **24**: 697.

Sharifnia, M., Eftekhari, Z. and Mortazavi, P., 2023. Niosomal hesperidin attenuates the M1/M2-macrophage polarization-based hepatotoxicity followed chlorpyrifos-induced toxicities in mice. *Pestic. Biochem. Physiol.*, 105724. https://doi.org/10.21203/rs.3.rs-3123664/v1

Shi, Z., Mahdavian, Y., Mahdavian, Y., Mahdigholizad, S., Irani, P., Karimian, M., Abbasi, N., Ghaneialvar, H., Zangeneh, A. and Zangeneh, M.M., 2021. Cu immobilized on chitosan-modified iron oxide magnetic nanoparticles: Preparation, characterization and investigation of its anti-lung cancer effects. *Arab. J. Chem.*, **14**: 103224. https://doi.org/10.1016/j.arabjc.2021.103224

Sultan, N., Amin, L.E., Zaher, A.R., Grawish, M.E., Scheven, B.A., 2021. Dental pulp stem cells stimulate neuronal differentiation of PC12 cells. *Neural Regen. Res.*, **16**: 1821–1828. https://doi.org/10.4103/1673-5374.306089

Wiatrak, B., Kubis-Kubiak, A., Piwowar, A. and Barg, E., 2020. PC12 cell line: Cell types, coating of culture vessels, differentiation and other culture conditions. *Cells*, **9**. https://doi.org/10.3390/cells9040958

Yang, C.Y., Huang, W.Y., Chen, L.H., Liang, N.W., Wang, H.C., Lu, J., Wang, X. and Wang, T.W., 2021. Neural tissue engineering: The influence of scaffold surface topography and extracellular matrix microenvironment. *J. Mater. Chem. B*, **9**: 567–584. https://doi.org/10.1039/D0TB01605E

Yousefi, T.S., Mehrzad, J. and Dehghani, H., 2021. Effect of glutamine stability on the long-term culture and line establishment of chicken primordial germ cells. *J. Cell Mol. Res.*, **13**: 44–53.